

INVESTIGATION OF THE MAGNETIC CHICANE OF THE SHORT-PULSE FACILITY AT THE DELTA STORAGE RING *

R. Molo †, J. Grewe, M. Höner, H. Huck, M. Huck, S. Khan, A. Schick, P. Ungelenk,
Center for Synchrotron Radiation (DELTA), TU Dortmund University, Dortmund, Germany

Abstract

The new short-pulse facility at the 1.5-GeV synchrotron light source DELTA based on coherent harmonic generation (CHG) utilizes an electromagnetic undulator which can be configured as an optical klystron (undulator - chicane - undulator). To optimize the CHG signal, the energy modulation of the electrons in the first undulator and the longitudinal dispersion of the magnetic chicane (i.e. the R_{56} matrix element) have to be optimized. Since the R_{56} value of the hitherto existing chicane was not sufficient, a more efficient dispersive section was created by rewiring the respective magnetic coils. Simulations of the previous and present chicane will be compared to measurements of the R_{56} matrix element, which show that the new arrangement increases the R_{56} value by a factor of ten.

INTRODUCTION

DELTA is a 1.5-GeV synchrotron light source operated by the TU Dortmund University. The new source for ultra-short VUV pulses [1] is based on coherent harmonic generation (CHG) [2] utilizing an electromagnetic undulator (U250) which can be configured as an optical klystron, i.e. two undulators separated by a magnetic chicane. The chicane converts the laser-induced energy modulation created in the first undulator (modulator) into a density modulation (microbunching). In the second undulator (radiator), the microbunches radiate coherently at the seeding wavelength λ_l and harmonics thereof.

The ratio of the coherent power P_c and the incoherent power P_i radiated by the whole bunch is given by [3]

$$\frac{P_c}{P_i} \approx g(N, \tau_b, \tau_l) \cdot b_n(\lambda_l)^2, \quad (1)$$

where N is the number of electrons in the bunch, τ_b is the bunch length (FWHM), τ_l is the laser pulse length (FWHM) and $b_n(\lambda_l)$ is the so-called bunching factor for a given harmonic n of the initial laser wavelength λ_l . A reasonable estimate for the function g is

$$g(N, \tau_b, \tau_l) \approx N \left(\frac{\tau_l}{\tau_b} \right)^2 \quad (2)$$

and the bunching factor reads (one-dimensional model) [3]

$$b_n(\lambda_l) = J_n(n R_{56} k A) \cdot \exp\left(-\frac{1}{2} (n R_{56} k \sigma_{rel})^2\right), \quad (3)$$

where R_{56} is the matrix element of the chicane describing its longitudinal dispersion [4], $A \equiv \Delta E/E$ is the energy modulation amplitude relative to the beam energy E , σ_{rel} is the relative energy spread and $k = 2\pi/\lambda_l$.

To optimize the CHG signal, the relative energy modulation A of the electrons in the first undulator should match the R_{56} value of the magnetic chicane satisfying the approximate relation

$$\frac{\lambda_l}{4} \approx R_{56} A, \quad (4)$$

where A is limited by the energy acceptance given by either the RF system or the transverse aperture of the storage ring. In the case of DELTA, the maximum is $A_{max} = 0.8\%$. The previous chicane was limited to $R_{56} \approx 11 \mu\text{m}$, which is not sufficient to fulfill Eq. (4) for the seed wavelengths $\lambda_l = 800 \text{ nm}$ or $\lambda_l = 400 \text{ nm}$.

Since the chicane is not constructed from standard dipole magnets but closely placed undulator poles, the magnetic field $B(s)$ is a continuously changing function of s , and the following formula has to be used [5, 6]

$$R_{56} = \left(\frac{L}{\gamma^2} + \left(\left(\frac{e}{c m_0 \gamma} \right)^2 \int_0^s \left[\int_0^{s'} B(\bar{s}) d\bar{s} \right]^2 ds' \right) \right), \quad (5)$$

where L is the length of the chicane, γ is the Lorentz factor, e is the elementary charge, m_0 is the electron rest mass and c is the speed of light.

A symmetric optical klystron configuration (i.e. the first and second undulator are tuned to the same wavelength) allows to measure the R_{56} value of the chicane. Due to interference between the two undulators, the spectrum can be described by [7]

$$I_{ok}(\lambda) = 2I_u \left(1 + f \cos \left(2\pi (N_u + N_d) \frac{\lambda - \lambda_r}{\lambda} \right) \right), \quad (6)$$

where N_u is the number of undulator periods and λ_r the resonant wavelength. The parameter N_d characterizes the strength of the chicane and is connected to R_{56} by

$$N_d = \frac{R_{56}}{2\lambda_r}. \quad (7)$$

The spectrum of one undulator is

$$I_u \propto \left(\frac{\sin \left(\pi N_u \frac{\lambda - \lambda_r}{\lambda} \right)}{\pi N_u \frac{\lambda - \lambda_r}{\lambda}} \right)^2 \quad (8)$$

* Work supported by DFG, BMBF, and the Federal State NRW.

† robert.molo@tu-dortmund.de

and the modulation depth is

$$f = f_0 \exp\left(-8\pi^2((N_u + N_d)\sigma_{rel})^2\right), \quad (9)$$

where $f_0 \approx 1$ is related to the spectrometer resolution.

SIMULATION

The magnetic field $B(s)$ of the chicanes was simulated for a maximum coil current of 800 A with the electromagnetic field simulation code CST Microwave Studio [8]. The magnetic field of the configurations sketched in Fig. 1 is shown in Fig. 2 as function of the longitudinal position s . In the previous configuration, the chicane, the modulator and the radiator used end poles with 1/4 and 3/4 of the full field in order to minimize the first and second field integral. The present chicane is a symmetric configuration minimizing the field integrals without additional matching poles, but now the polarity of the second undulator is reversed and the second and fifth pole of the chicane are used to reduce the field integrals of the modulator and radiator.

Equation (5) allows to calculate the R_{56} value as function of the position along the chicane as shown in Fig. 3. The symmetric chicane significantly increases the R_{56} value and allows to reach the optimum microbunching which not only yields the maximum CHG signal but also allows to measure the energy modulation induced by the laser pulse.

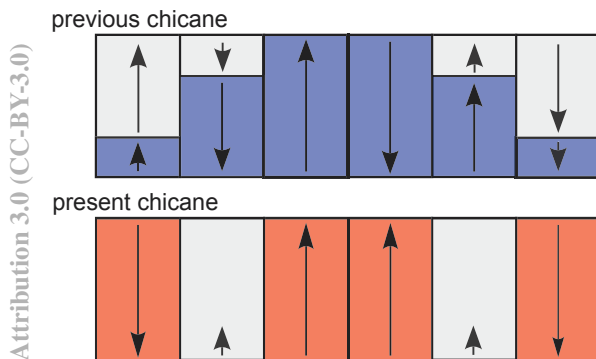


Figure 1: Configuration of the antisymmetric (previous) and symmetric (present) magnetic chicane at DELTA comprising 6 magnetic coils. The length of each arrow represents the fraction of the maximum coil current and its direction indicates the polarity of the magnetic field. The colored blocks illustrate the poles of the chicanes and the gray blocks denote the matching poles for the modulator and radiator.

MEASUREMENTS

R_{56} Values of the Chicane

The R_{56} values of the chicanes were measured by recording spectra of the radiation generated by the U250 optical klystron with both undulators tuned to 400 nm. An

ISBN 978-3-95450-122-9

1890

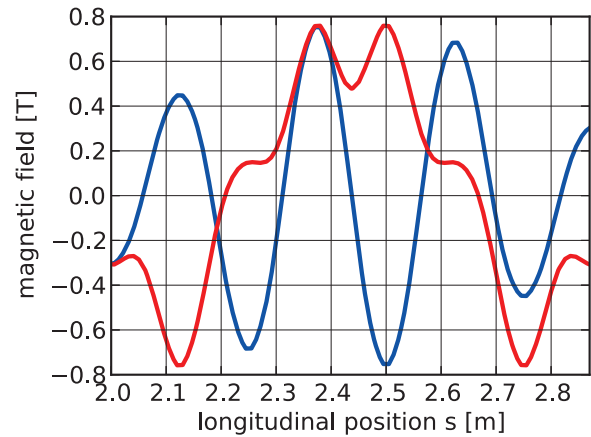


Figure 2: Simulation of the magnetic field of the symmetric (red) and antisymmetric (blue) chicane for a maximum coil current of 800 A.

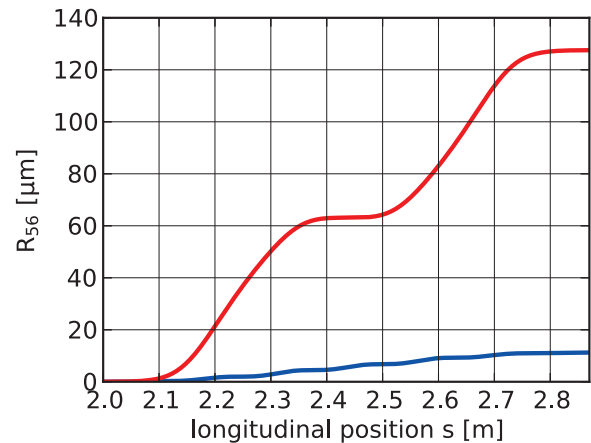


Figure 3: Simulation of the R_{56} value versus longitudinal position along the symmetric (red) and antisymmetric (blue) chicane for a maximum coil current of 800 A.

example is depicted in Fig. 4 showing the typical interference pattern. Even slight changes of the chicane current modify this pattern, which allows to determine the R_{56} value by fitting Eq. (6) to the spectra. The resulting R_{56} values as function of the chicane current are shown in Fig. 5 appearing even higher than expected from the simulation. A possible reason is the uncertainty of the iron permeability used in the CST model. Due to the limited resolution of the spectrometer, the R_{56} values of the new chicane for currents above 700 A cannot be measured. The offset of $2.6 \mu\text{m}$ at zero current can be explained by the matching poles for the modulator and radiator which generate dispersion.

Energy Modulation

Figure 6 shows the measured ratio of the coherent signal P_c and the incoherent signal P_i produced by the whole

05 Beam Dynamics and Electromagnetic Fields

D01 Beam Optics - Lattices, Correction Schemes, Transport

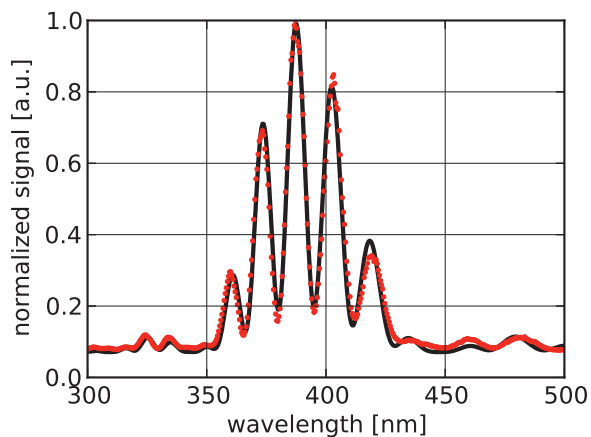


Figure 4: Measured spectrum of the U250 optical klystron tuned to 400 nm with a chicane current of 150 A. The black curve is a fit based on Eq. (6).

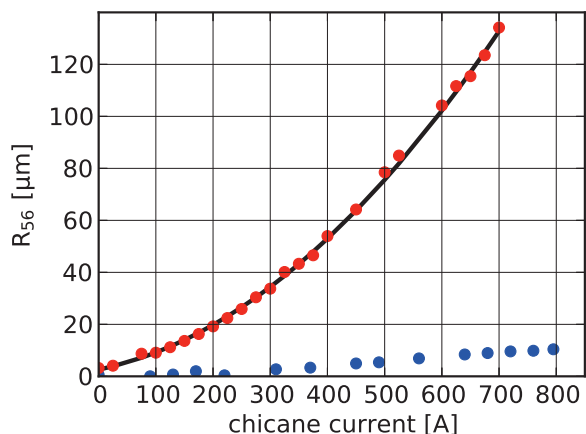


Figure 5: Measured R_{56} values versus chicane current for the present (red) and previous (blue) chicane. The black curve is a quadratic fit to the R_{56} values of the present chicane.

bunch. Due to the new symmetric chicane, the coherent CHG signal reaches a maximum at $R_{56} = 23 \mu\text{m}$ with a ratio of 200 and more, which would be impossible with the previous chicane. Fitting Eq. (1) to the data allows to determine an “effective” energy modulation of $A \approx 0.33\%$ averaged over a modulation with Gaussian envelope.

CONCLUSIONS

The chicane of the U250 optical klystron was significantly modified during the winter shutdown 2012 by rewiring the 6 chicane poles. The new chicane increases the possible R_{56} value from $11 \mu\text{m}$ to about $130 \mu\text{m}$ which in turn allows to measure the laser-induced energy modulation of the electrons. The presented theory and simulations fit well to the measured data.

Simulations including three-dimensional effects [9] re-

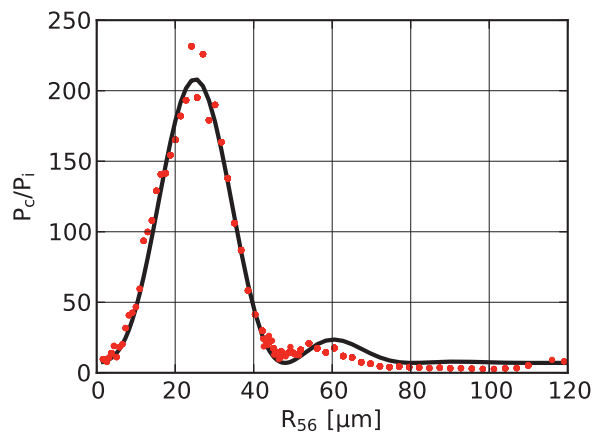


Figure 6: Measured ratio P_c/P_i for the second harmonic of 400 nm versus R_{56} of the present chicane. The black curve is a fit based on the one-dimensional theory (Eq. (1)). In this example, $P_c/P_i \approx 200$ was obtained.

veal that the effective energy modulation should reach about 0.6% if the laser parameters are optimized. During this measurement, the effective energy modulation was 0.33% indicating that the laser configuration and setup (telescope, pulse length, intensity) can be optimized further in order to improve the laser-electron interaction.

In practice, the energy modulation can be optimized by changing laser parameters while scanning the chicane current. For each setting, Eq. (1) allows to determine the relative energy modulation.

ACKNOWLEDGMENT

It is a pleasure to thank our colleagues at DELTA and the Faculty of Physics for their continuous support. The project has profited from the expertise of Günter Dahlmann, Bernard Riemann and Helge Rast.

REFERENCES

- [1] M. Huck et al., this conference (WEPWA005).
- [2] R. Coisson and F. D. Martini, Phys. of Quant. Electron. 9, 939 (1982).
- [3] J. Wu and L. H. Yu, SLAC-PUB 10494 (2004).
- [4] H. Wiedemann, Particle Accelerator Physics (Springer 2008).
- [5] Y. Li and J. Pflueger, Proc. of FEL 2010, Malmö, 652.
- [6] R. Molo, Diploma Thesis, TU Dortmund, 2011.
- [7] P. Elleaume, Le Journal de Physique Colloques 44.C1, 333 (1983).
- [8] CST Microwave Studio, www.cst.com.
- [9] M. Höner et al., Proc. of IPAC 2011, San Sebastian, 2939.